



Short communication

# Wettability and photocatalysis of CF<sub>4</sub> plasma etched titania films of honeycomb structure

Do-Yeon Kim<sup>a</sup>, Jung-Jae Park<sup>a</sup>, Jong-Gun Lee<sup>a</sup>,  
Maikel F.A.M. van Hest<sup>b</sup>, Sam S. Yoon<sup>a,\*</sup>

<sup>a</sup>School of Mechanical Engineering, Korea University, Seoul 136-713, Korea

<sup>b</sup>National Renewable Energy Laboratory, Golden, Colorado 80401, USA

Received 9 March 2013; received in revised form 25 April 2013; accepted 25 April 2013

Available online 14 May 2013

## Abstract

We prepared titania films by aerosol deposition (AD), in which titania powder is supersonically accelerated for deposition onto a substrate. These AD titania films exhibited hydrophilicity and photocatalysis under UV exposure. However, after surface modification by CF<sub>4</sub> plasma-etching, the films showed higher hydrophilicity and lower photocatalytic effect. After sufficient modification, they exhibited superhydrophilicity, which was induced by the presence of fluorine. This type of surface modification is useful for promoting hydrophilicity under no UV light exposure.

© 2013 Elsevier Ltd and Techna Group S.r.l. All rights reserved.

**Keywords:** D. TiO<sub>2</sub>; Aerosol deposition; CF<sub>4</sub> etching; UV-light; Superhydrophilic

## 1. Introduction

Semiconducting metal oxides, such as ZnO, SnO<sub>2</sub>, and TiO<sub>2</sub>, possess excellent photocatalytic and hydrophilic properties when they are exposed to ultra-violet (UV) light. These UV-induced effects are used in many practical applications, e.g. self-cleaning, deodorizing, self-sterilizing, air-cleaning, and anti-fogging products [1]. Among the metal oxides, TiO<sub>2</sub> has been considered the most popular photocatalytic material because of its availability, chemical stability, low cost, non-toxicity, biocompatibility, and recyclability [1–4]. Because of these advantages, TiO<sub>2</sub> has been also used in water-splitting electrodes and dye-sensitized solar cells [5]. TiO<sub>2</sub> have two distinct characteristics of photocatalysis and hydrophilicity. When they are exposed to light whose energy exceeds the band gap energy, its electrons are excited and transferred from the valence band to the conduction band. The photo-induced electrons and holes react with electron acceptors and donors to produce hydroxyl radicals.

The hydrophilicity of TiO<sub>2</sub> originates from the OH radicals that are produced from the reaction between the photogenerated holes and water. This reaction also produces Ti<sup>3+</sup> and oxygen vacancies, which in turn adsorb water molecules at defect sites to further promote hydrophilicity. On the other hand, in photocatalysis, photo-induced generated reactive oxygen species like hydroxyl radicals, hydrogen peroxide, and superoxide work together to decompose or oxidize various organic and inorganic compounds [6]. TiO<sub>2</sub>'s strong oxidizing capabilities are especially useful for realizing water purification applications that are economically viable and environmentally friendly. A TiO<sub>2</sub> catalyst can be recycled indefinitely without additional chemical treatment [7–10].

Interestingly, even hydrophobicity can be promoted by roughening the surface of TiO<sub>2</sub> films via plasma-etching [2], and via a mechanism explained by the Cassie–Baxter state [11]. Zhang et al. [2] roughened a smooth sol–gel TiO<sub>2</sub> films produced by sol–gel coating. Then CF<sub>4</sub> plasma etching was applied to obtain a nano-columnar structure. Under UV illumination, the plasma-etched hydrophobic surface converted into a hydrophilic surface. The air trapped between the nano-scale columnar structures enabled hydrophobicity due to the Cassie–Baxter state. Conversely, hydrophilicity due to the

\*Corresponding author.

E-mail address: [skyoona@korea.ac.kr](mailto:skyoona@korea.ac.kr) (S.S. Yoon).

Wenzel state [12] was obtained under UV exposure despite the nanocolumnar structures.

Interestingly, the effect of plasma-etching of a TiO<sub>2</sub> film surface with micrometer-scale roughness such as aerosol-deposited films, Kim et al. [13], is completely different from that of a TiO<sub>2</sub> film surface with nanometer-scale roughness, as observed by Zhang et al. [2]. For a micrometer-rough surface, the air trapping effect of the Cassie–Baxter state is minimized, and the chemical surface modification via CF<sub>4</sub> plasma etching dominates [13]. The CF<sub>4</sub> plasma replaces the surface oxygen with fluorine, which is highly electro-negative, to promote the adsorption of water molecules, making the film surface hydrophilic even without UV light illumination [13]. This type of surface modification may be useful for cases requiring hydrophilicity, especially when a UV light source is not available.

To the best of our knowledge, there has been no study on the variation of the contact angle (which is a measure of hydrophilicity) as a function of UV light exposure duration for plasma-etched titania films with micrometer-scale roughness. This type of measurement of hydrophilicity is needed to evaluate the photo-sensitivity of a plasma-etched film. It is expected that a TiO<sub>2</sub> film with complete surface modification will be permanently hydrophilic even without UV light illumination. An aerosol-deposited titania film acquires superhydrophilicity after CF<sub>4</sub> plasma-etching, but its photocatalysis, the other distinct behavior of titania, may be changed by the severe surface modification. Therefore, this change in photocatalytic characteristic must be evaluated quantitatively. In this study, the photocatalytic performances of titania films modified for various etching times are evaluated.

## 2. Experimental setup

The aerosol deposition (AD) experimental setup consisted of an air tank, fluidized-bed powder feeder, nozzle, vacuum chamber, 2D *x*–*y* stage, booster pump, and vacuum pump; see Fig. 1. Titania powder was a mixture of 60% anatase and 40% rutile by weight. Agglomeration was observed. To break up the particle clusters, the powder was mixed with water and put into a rotary evaporator, calcinated at 400 °C, and then ball-milled for 24 h. This break-up process resulted in particles having an average size of approximately 0.5 μm. Such pre-treatment is expected to improve the deposition rate [14]. Further details of our experimental setup can be found elsewhere [13,15]. Experimental conditions are summarized in Table 1.

All titania films were deposited at room temperature on soda-lime glass substrates with surface areas and roughness of 2.5 × 2.5 cm<sup>2</sup> and *R*<sub>a</sub> < 5 nm, respectively. The substrates were cleaned in an ultrasonic acetone bath and completely dried in open atmospheric condition at room temperature before use.

Table 1  
Typical deposition conditions.

|                                       |            |
|---------------------------------------|------------|
| Pressure in deposition chamber [Torr] | 0.35–5.6   |
| Propellant gas                        | Air        |
| Nozzle exit area [mm <sup>2</sup> ]   | 10 × 35    |
| Stand-off distance [mm]               | 5          |
| Gas temperature                       | RT (20 °C) |
| Consumption of propellant gas [l/min] | 10         |
| Stage traverse speed [mm/s]           | 0.72       |
| Number of passes                      | 4          |

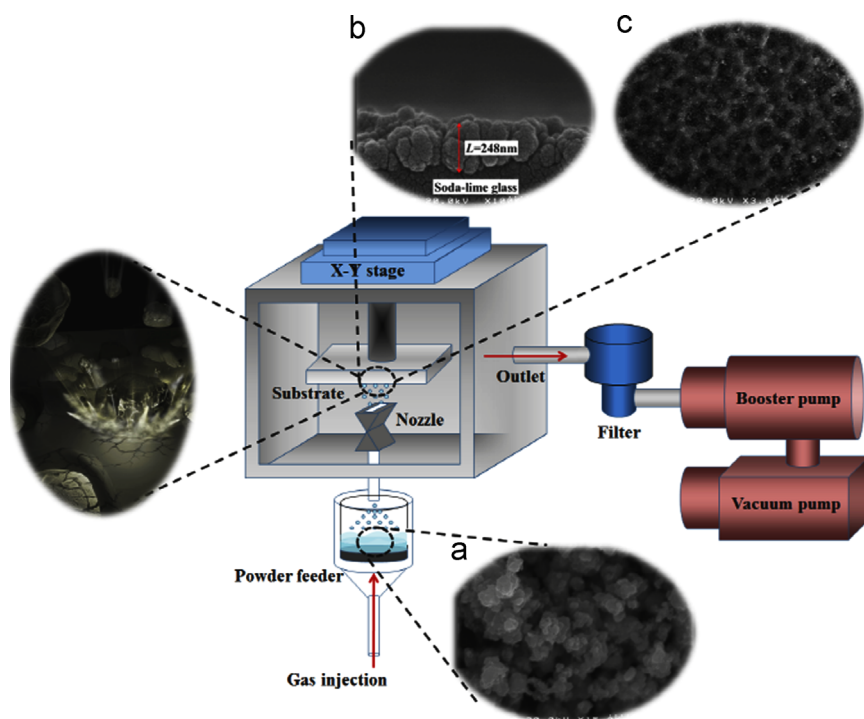


Fig. 1. Schematic of the experimental setup (a) SEM of the TiO<sub>2</sub> powder, (b) side and (c) top views of an AD TiO<sub>2</sub> film.

The microstructures and crystallinity of the deposited titania films were characterized by high-resolution scanning electron microscopy (HRSEM, XL30SFEG Phillips Co., the Netherlands at 10 kV). Elemental concentration and oxidation states were measured by X-ray photoelectron spectroscopy (XPS, VG Multilab ESCA 2000 system, Waltham, UK).

Titania films (each sample was  $2.5 \times 2.5 \text{ cm}^2$ ) were placed inside the deposition chamber and plasma-etched with  $\text{CF}_4$  reactive gas (50 sccm, 100 W, and 15 mTorr) for etching times ranging from  $t_{\text{etch}}=0$  to 6 min at intervals of  $\Delta t_{\text{etch}}=2$  min. The plasma-etching system pressure was maintained at  $5.0 \times 10^{-5}$  Torr. A radio frequency of 13.56 MHz was applied to the bottom electrode of the chamber, which was maintained at  $20^\circ\text{C}$ .

Before contact angle measurement, all titania films were kept inside a dark box in an inert environment for two days, after which each film was illuminated inside a UV light box ( $0.6 \text{ mW/cm}^2$  UV exposure in  $22^\circ\text{C}$  air with relative humidity at 80%) for various UV exposure durations. The contact angle of each film was measured using an ultra-pure water droplet ( $20 \text{ M}\Omega$  resistivity at  $20^\circ\text{C}$ ) of 2 mm diameter, which was placed on the film. The interval between a film being taken outside the UV box and the contact angle measurement was less than 1 min, minimizing exposure to laboratory light. For reliability, the average of three test measurements was used as the final contact angle value.

Methylene blue (MB) solutions have often been used as model pollutants for determining photocatalytic effect. They decompose by direct oxidation and by reaction with OH radicals generated during a photocatalytic process [16,17]. An MB solution (#M2661, whose initial weight concentration was 0.1 wt% in water, *Samchun Chemical*, Korea) was mixed with deionized water at 1:400 volume ratio; 200 ml of DI water and 0.5 ml of MB solution were mixed together. A titania film was placed inside a Pyrex vessel and sealed with a Pyrex Petridish. The concentration of MB inside the vessel decreased as photocatalysis proceeded, as monitored by a UV–vis spectrophotometer (OPTIZEN POP, *Mecasys Co. Ltd.*, Korea,  $=190 \leq \lambda \leq 1100 \text{ nm}$ ). Absorbance data from the UV–vis spectroscopy were obtained by converting the transmittance data using the Lambert–Beer law [18,19].

### 3. Results and discussion

Fig. 2 shows a typical honeycomb surface structure of an aerosol deposited titania film. This honeycomb microstructure

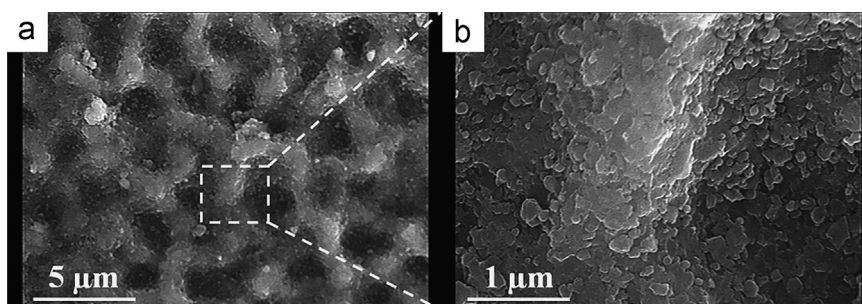


Fig. 2. (a) An SEM image of an AD titania film showing the 3D cross-linked honeycomb structure and (b) its magnified view.

was self-assembled, although the previous authors had intentionally designed this three-dimensional cross-linked structure [13,20–23], which is favorable for applications requiring maximum surface area.

Fig. 3 shows the variations of contact angle according to etching time ( $t_{\text{etch}}$ ) and UV duration ( $t_{\text{UV}}$ ).  $\text{CF}_4$  plasma etching roughens both smooth [2] and nanometer-scale rough surfaces [24]. However, plasma etching does not significantly change the micrometer-scale rough surfaces (e.g., aerosol-deposited titania films); rather, chemical surface modification is dominant. Therefore, nanometer-scale physical erosion due to plasma-etching will not be apparent in the aerosol-deposited films, where micrometer-scale features are dominant. This is different from the case of Zhang et al. [2] who showed the creation of nanometer-scale pinholes by plasma-etching along the grain boundaries of a dip-coated smooth titania surface. In their experimental studies, the nanocolumnar structure was physically eroded by plasma-etching, resulting in the formation of nanocolumns of  $\sim 20 \text{ nm}$  diameter and  $\sim 80 \text{ nm}$  height. Between these nanocolumns, air pockets were trapped in the pinholes, providing a hydrophobic surface of the Cassie–Baxter state [11] in the absence of the UV light. Upon exposure to UV light, the photogenerated holes absorbed water to produce OH radicals. This reaction produced  $\text{Ti}^{3+}$  and oxygen vacancies, which in turn adsorbed water molecules at defect sites to further promote hydrophilicity.

On the other hand, the aerosol-deposited surface consisted of the honeycomb structure, which has surface features of  $1\text{--}2 \mu\text{m}$  diameter and roughness of  $50 \text{ nm} \leq R_a \leq 100 \text{ nm}$ , according to AFM measurements [1]. The effect of plasma-etching on the surface morphology was not apparent, at least microscopically [13]. Nevertheless, the contact angles varied when the films were subjected to longer plasma etching times, as shown in Fig. 3.

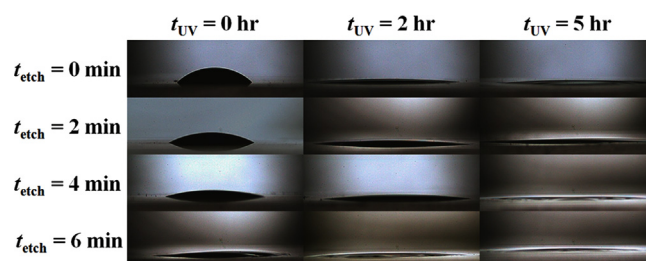


Fig. 3. The contact angle variation as functions of etching time ( $t_{\text{etch}}$ ) and UV duration ( $t_{\text{UV}}$ ).

The mechanism of these low contact angles of the plasma-etched films is explained by the presence of fluorine, whose electro-negativity promoted hydrophilicity [13].

Fig. 4 quantitatively shows the variation of the contact angle as a function of etching and UV illumination times. It is apparent that longer UV illumination durations lead to smaller contact angles for all films. Furthermore, the initial contact angle at  $t_{UV}=0$  is lower for longer  $CF_4$  etching durations, indicating that increasing fluorine content increases the wettability of a film. However, the as-deposited AD film ( $t_{etch}=0$ ) shows the largest contact angle variations, while the plasma-etched films show relatively moderate contact angle variations. This trend indicates the competition or tradeoff between UV-driven hydrophilicity and hydrophilicity of fluorine-modified plasma-etching. The data suggest that photo-induced hydrophilicity can be completely removed if  $t_{etch}$  is increased beyond 6 min. Note that UV-driven hydrophilicity is more effective after 2 h of UV illumination for the as-deposited film than for the films produced with  $t_{etch}=2$  and 4 min. Therefore  $CF_4$  etching of a  $TiO_2$  film will not always result in the lowest contact angle even if UV sources are abundant. After  $t_{UV}=2$  h, most of the films reached the state of superhydrophilicity (a contact angle of 5 degrees or less).

Fig. 5 shows XPS data for the films with and without UV exposure for different  $CF_4$  etching times. A clear fluorine signal is seen for the films that were etched, with the strongest signal for the film etched for the longest time. No distinction in XPS signal is observed between the films with and without UV exposure, indicating that UV light did not influence the compositions of the films.

Besides the variations of the contact angles of the  $TiO_2$  films due to  $CF_4$  plasma etching, the photocatalytic effects of the films were determined using a methyleneblue solution (MB). In Fig. 6, the absorption of the MB solution by the different  $TiO_2$  films under UV light exposure for 2 h is shown. The as-deposited  $TiO_2$  film shows the largest decrease in absorption,

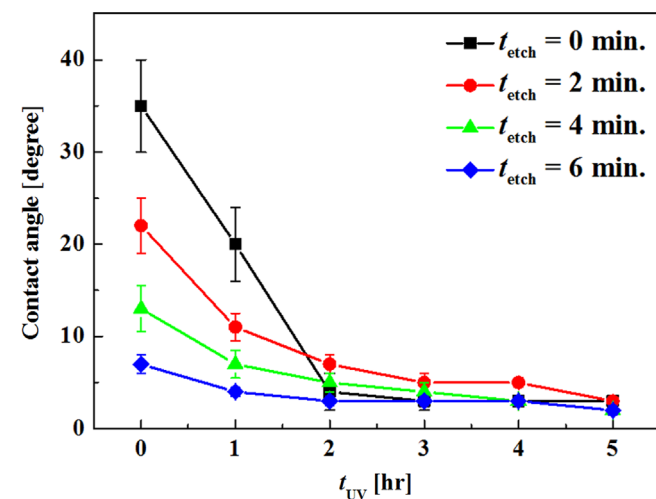


Fig. 4. Contact angles as a function of the UV irradiation time for the films fabricated at various etching times ( $t_{etch}=2, 4, 6$ , and 8 min). The film thickness was in the range of 2.5–3.0  $\mu m$ . The as-deposited film without  $CF_4$  plasma-etching is indicated with  $t_{etch}=0$  min.

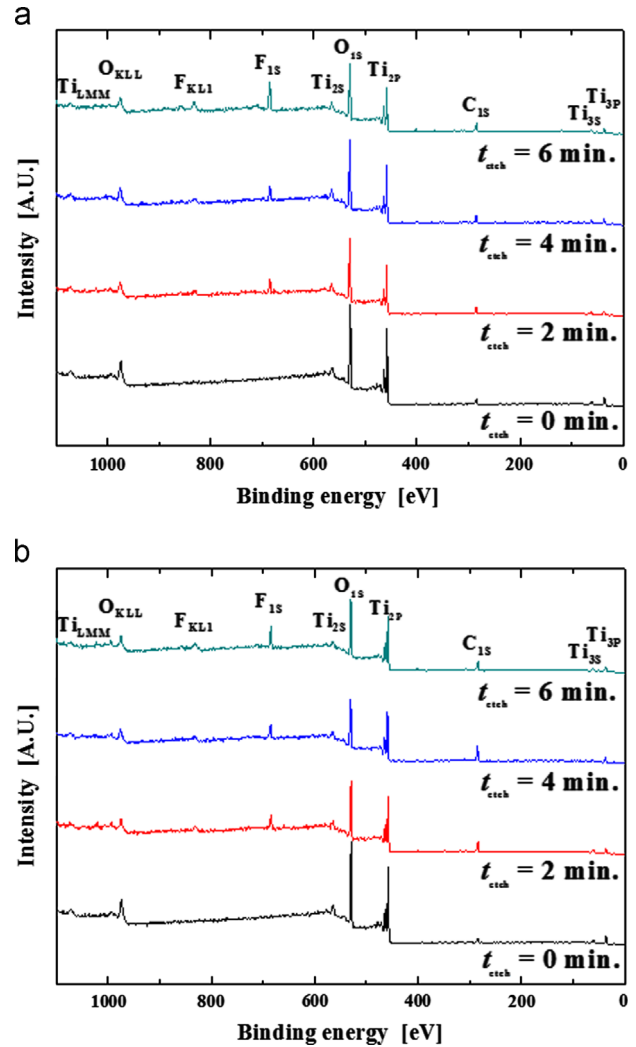


Fig. 5. XPS results for various etching times (a) without UV-light and (b) with UV-light.

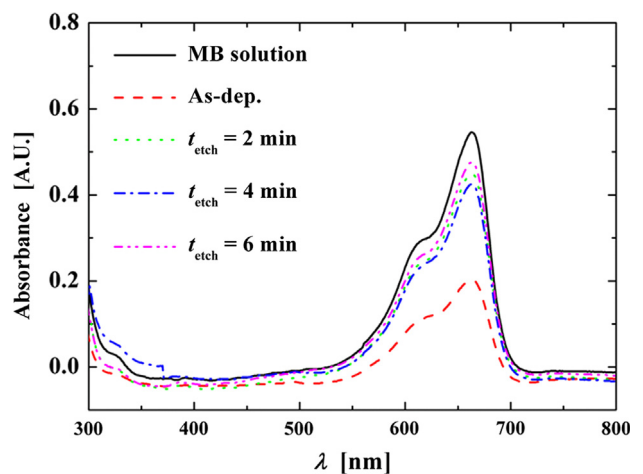


Fig. 6. Effect of UV exposure on MB photodegradation. UV-vis spectra of the MB solution (0.1 wt% solution in deionized water) with the plasma-etched  $TiO_2$  films plasma-etched at various etching time. The films were irradiated for 2 h (0.6 mW/cm<sup>2</sup> UV exposure in 22 °C air with relative humidity at 80%).

indicating the strongest photocatalytic effect, and the CF<sub>4</sub> etched TiO<sub>2</sub> films show very small changes in absorption, suggesting that incorporation of fluorine in the films inhibited the normal reaction mechanism of MB on the TiO<sub>2</sub> surfaces under UV exposure. It is well known that the mechanism of MB decomposition reaction is initiated by a UV generated free electron from the TiO<sub>2</sub> [19,25,26]:



with the free electron generated by the absorption of a UV photon in the TiO<sub>2</sub>



MB<sup>\*-</sup> is unstable and will readily react with oxygen and decompose MB into HCl, HSO<sub>4</sub>, HNO<sub>3</sub>·CO<sub>2</sub> and H<sub>2</sub>O. In pure TiO<sub>2</sub> films, any free electron can reach the surface of the film, where it can initiate the reaction. However, in CF<sub>4</sub> plasma etched films, the fluorine will ‘capture’ the free electron because of its strong electro-negativity, preventing the transfer of the free electron to the MB, which interacts with the film surface. Without the electron transfer to the MB, MB cannot dissociate and thus break-down; therefore, a CF<sub>4</sub> etched TiO<sub>2</sub> film will not be photocatalytic. The longer the etching time, the higher the fluorine concentration in the TiO<sub>2</sub> film, as indicated by the absorption change of the MB solution, which is the smallest for the longest etching time. By optimizing the etching process, it may be possible to separately control the photocatalytic effect and hydrophilicity of TiO<sub>2</sub> films.

#### 4. Conclusion

This study compared the hydrophilicity and photocatalysis of CF<sub>4</sub> plasma etched and unetched titania films fabricated by aerosol deposition, in which titania powder is supersonically accelerated for deposition onto a substrate. The AD titania films consisted of the self-assembled honeycomb structure, which was three-dimensional and highly cross-linked. This structure may be useful for applications requiring a maximal surface area. The films fabricated by 6-min of etching exhibited superhydrophilicity under minimal UV light exposure, while the as-deposited film needed at least 2 h of UV light exposure in order to exhibit a similar level of superhydrophilicity. On the other hand, the as-deposited film showed the maximal photocatalytic performance while the plasma-etched films showed the minimal performance. Longer plasma-etching durations led to lower photocatalytic performances. Thus there is a clear tradeoff between hydrophilicity and photocatalysis in CF<sub>4</sub> plasma-etched titania films.

#### Acknowledgment

This work was supported by the Center for Inorganic Photovoltaic Materials (NRF-2013-0001169) funded by the Korean government (MEST), 2010K000969, B551179-08-03-00, and KUCE Crimson Professorship.

#### References

- [1] J.J. Park, J.G. Lee, D.Y. Kim, J.H. Hong, J.J. Kim, S. Hong, S.S. Yoon, Antibacterial and water purification activities of self-assembled honeycomb structure of aerosol deposited titania film, *Environmental Science and Technology* 46 (2012) 12510–12518.
- [2] X. Zhang, M. Jin, Z. Liu, D.A. Tryk, S. Nishimoto, T. Murakami, A. Fujishima, Superhydrophobic TiO<sub>2</sub> surfaces: preparation, photocatalytic wettability conversion, and superhydrophobic–superhydrophilic patterning, *Journal of Physical Chemistry C* 111 (2007) 14521–14529.
- [3] S.D. Richardson, A.D. Thruston Jr, T.W. Collette, K.S. Patterson, B.W. Lykins Jr, J.C. Ireland, Identification of TiO<sub>2</sub>/UV disinfection byproducts in drinking water, *Environmental Science and Technology* 30 (1996) 3327–3334.
- [4] B.R. Eggins, F.L. Palmer, J.A. Byrne, Photocatalytic treatment of humic substances in drinking water, *Water Research* 31 (1997) 1223–1226.
- [5] S. Fan, G. Yang, C. Li, G. Liu, C. Li, L. Zhang, Characterization of microstructure of nano-TiO<sub>2</sub> coating deposited by vacuum cold spraying, *Journal of Thermal Spray Technology* 15 (2006) 513–517.
- [6] S.Y. Lu, D. Wu, Q.L. Wang, J. Yan, A.G. Buekens, K.F. Cen, Photocatalytic decomposition on nano-TiO<sub>2</sub>: destruction of chloroaromatic compounds, *Chemosphere* 82 (2011) 1215–1224.
- [7] T. Watanabe, S. Fukayama, M. Miyauchi, A. Fujishima, K. Hashimoto, Photocatalytic activity and photoinduced wettability conversion of TiO<sub>2</sub> thin film prepared by sol–gel process on a soda-lime glass, *Journal of Sol–Gel Science and Technology* 19 (2000) 71–76.
- [8] K. Hashimoto, H. Irie, A. Fujishima, TiO<sub>2</sub> photocatalysis: a historical overview and future prospects, *Japanese Journal of Applied Physics* 44 (Part 1) (2005) 8269.
- [9] K.-i. Ishibashi, Y. Nosaka, K. Hashimoto, A. Fujishima, Time-dependent behavior of active oxygen species formed on photoirradiated TiO<sub>2</sub> films in air, *Journal of Physical Chemistry B* 102 (1998) 2117–2120.
- [10] K. Ikeda, H. Sakai, R. Baba, K. Hashimoto, A. Fujishima, Photocatalytic reactions involving radical chain reactions using microelectrodes, *Journal of Physical Chemistry B* 101 (1997) 2617–2620.
- [11] A. Cassie, S. Baxter, Wettability of porous surfaces, *Transactions of the Faraday Society* 40 (1944) 546–551.
- [12] R.N. Wenzel, Resistance of solid surfaces to wetting by water, *Industrial and Engineering Chemistry* 28 (1936) 988–994.
- [13] D.Y. Kim, J.J. Park, J.G. Lee, M.W. Lee, H.Y. Kim, J.H. Oh, T.Y. Seong, D. Kim, S.C. James, M.F.A.M. Hest, Tuning hydrophobicity with honeycomb surface structure and hydrophilicity with CF<sub>4</sub> plasma etching for aerosol deposited titania films, *Journal of the American Ceramic Society* (2012).
- [14] J. Akedo, Aerosol deposition of ceramic thick films at room temperature: densification mechanism of ceramic layers, *Journal of the American Ceramic Society* 89 (2006) 1834–1839.
- [15] J.-J. Park, D.Y. Kim, J.G. Lee, D. Kim, J.-H. Oh, T.-Y. Seong, M.F. Hest, S.S. Yoon, Superhydrophilic transparent titania films by supersonic aerosol deposition, *Journal of the American Ceramic Society* (2013).
- [16] R.B. Draper, M.A. Fox, Titanium dioxide photosensitized reactions studied by diffuse reflectance flash photolysis in aqueous suspensions of TiO<sub>2</sub> powder, *Langmuir* 6 (1990) 1396–1402.
- [17] C.S. Turchi, D.F. Ollis, Mixed reactant photocatalysis: intermediates and mutual rate inhibition, *Journal of Catalysis* 119 (1989) 483–496.
- [18] K. Fuwa, B. Valle, The physical basis of analytical atomic absorption spectrometry, Pertinence of the Beer–Lambert Law, *Analytical Chemistry* 35 (1963) 942–946.
- [19] C. Yogi, K. Kojima, N. Wada, H. Tokumoto, T. Takai, T. Mizoguchi, H. Tamiaki, Photocatalytic degradation of methylene blue by TiO<sub>2</sub> film and Au particles-TiO<sub>2</sub> composite film, *Thin Solid Films* 516 (2008) 5881–5884.
- [20] J. Yu, X. Zhao, Q. Zhao, G. Wang, Preparation and characterization of super-hydrophilic porous TiO<sub>2</sub> coating films, *Materials Chemistry and Physics* 68 (2001) 253–259.
- [21] M. Faustini, L. Nicole, C. Boissiere, P. Innocenzi, C. Sanchez, D. Grosso, Hydrophobic, antireflective, self-cleaning, and antifogging sol–gel coatings:

- an example of multifunctional nanostructured materials for photovoltaic cells, *Chemistry of Materials* (2010) 4406–4413.
- [22] G.K. Mor, O.K. Varghese, M. Paulose, K. Shankar, C.A. Grimes, A review on highly ordered, vertically oriented TiO<sub>2</sub> nanotube arrays: fabrication, material properties, and solar energy applications, *Solar Energy Materials and Solar Cells* 90 (2006) 2011–2075.
- [23] Z. Liu, X. Zhang, S. Nishimoto, M. Jin, D.A. Tryk, T. Murakami, A. Fujishima, Highly ordered TiO<sub>2</sub> nanotube arrays with controllable length for photoelectrocatalytic degradation of phenol, *Journal of Physical Chemistry C* 112 (2008) 253–259.
- [24] X. Zhang, M. Jin, Z. Liu, S. Nishimoto, H. Saito, T. Murakami, A. Fujishima, Preparation and photocatalytic wettability conversion of TiO<sub>2</sub>-based superhydrophobic surfaces, *Langmuir* 22 (2006) 9477–9479.
- [25] A. Mills, S.L. Hunte, An overview of semiconductor photocatalysis, *Journal of Photochemistry and Photobiology A-Chemistry* 108 (1997) 1–36.
- [26] A. Houas, H. Lachheb, M. Ksibi, E. Elaloui, C. Guillard, J.M. Herrmann, Photocatalytic degradation pathway of methylene blue in water, *Applied Catalysis B: Environmental* 31 (2001) 145–157.